Experimental Neurology 316 (2019) 39–51

Contents lists available at ScienceDirect

Experimental Neurology

journal homepage: www.elsevier.com/locate/yexnr

Research paper

Depletion of microglia immediately following traumatic brain injury in the pediatric rat: Implications for cellular and behavioral pathology

Lauren A. Hanlon[a,c], Ramesh Raghupathi[a,b,**], Jimmy W. Huh[d,*]

[a] Program in Neuroscience, Graduate School of Biomedical Sciences and Professional Studies, Drexel University, Philadelphia, PA, United States of America
[b] Department of Neurobiology and Anatomy, Drexel University, Philadelphia, PA, United States of America
[c] Department of Neurosurgery, University of Pennsylvania Perelman School of Medicine, Philadelphia, PA, United States of America
[d] Department of Anesthesiology and Critical Care, Children's Hospital of Philadelphia, Philadelphia, PA, United States of America

ARTICLE INFO

Keywords:
Pediatric TBI
Microglia
Clodronate
Neurodegeneration
Spatial learning
Cortical activity

ABSTRACT

The inflammatory response is a significant component of the pathophysiology of pediatric traumatic brain injury. High levels of inflammatory mediators have been found in the cerebrospinal fluid of brain-injured children which have been linked to poor prognosis. Targeting aspects of the inflammatory response in the hopes of finding a viable post-injury therapeutic option has gained attention. Microglia are largely responsible for perpetuating the injury-induced inflammatory response but in the developing brain they play beneficial roles in both normal and disease states. Following closed head injury in the neonate rat, depletion of microglia with intracerebral injections of liposomes containing clodronate was associated with an increase in neurodegeneration in the early post-injury period (3 days) relative to those injected with empty liposomes suggestive of a decrease in clearance of dying cells. In sham-injured animals, microglia repopulated the clodrosome-mediated depleted brain regions over a period of 2–4 weeks and exhibited morphology typical of a resting phenotype. In brain-injured animals, the repopulated microglia in clodrosome-injected animals exhibited rod-like and amoeboid morphologies. However, fluoro-Jade B reactivity in these brain regions was more extensive than in empty liposome-injected animals suggesting that the active microglia may be unable to clear dying neurons. This was accompanied by an induction of hyperexcitability in the local cortical circuitry. Depletion of microglia within the white matter tracts and the thalamus did not affect the extent of injury-induced traumatic axonal injury. Increased neurodegeneration in the dorsal subiculum was not accompanied by any changes to injury-induced deficits in spatial learning and memory. These data suggest that activation of microglia may be important for removal of dying neurons in the traumatically-injured immature brain.

1. Introduction

Traumatic brain injury (TBI) remains one of the leading causes of morbidity and mortality in infants and children < 4 years or age (Anderson et al., 2005; Coronado et al., 2011; Emami et al., 2017; Faul et al., 2010; Langlois et al., 2005). Improvements in supportive care in the acute post-traumatic period over the past decade has resulted in decreased mortality (C.D.C., 2016) although survivors are faced with a lifetime of behavioral deficits. Among the many complications that manifest over the lifespan of survivors of infant TBI are impairments of learning and memory, language and executive function all of which are often associated with pathologic alterations in both white and gray matter (Anderson et al., 2009, 2011; Babikian et al., 2015; Catroppa and Anderson, 2004, 2006; Dennis et al., 2015; Ewing-Cobbs et al., 2006; Ewing-Cobbs et al., 2004; Power et al., 2007; Salorio et al., 2005; Tong et al., 2004; Wilde et al., 2005). The mechanisms underlying these pathologic alterations are incompletely understood although activation of microglia leading to the synthesis and release of cytokines and chemokines, may play an important role (Loane and Kumar, 2016; Woodcock and Morganti-Kossmann, 2013). Following severe TBI in children, increase in pro- and anti-inflammatory cytokines such as interleukin (IL)-1β, IL-6, and IL-10, chemokines IL-8 and C—C motif ligand-3, and nucleotide-binding domain-like receptor protein-mediated inflammasome, and quinolinic acid, ferritin and soluble cluster of differentiation 163 (sCD163), indicative of microglia/macrophage activation in the cerebrospinal fluid has been observed (Bell et al., 1997;

* Corresponding author at: Department of Anesthesiology and Critical Care, Children's Hospital of Philadelphia, Wood Building 6th Floor- Rm. 6035, 3400 Civic Center Blvd, Philadelphia, PA 19104, USA.
** Corresponding author at: Department of Neurobiology and Anatomy, Drexel University College of Medicine, 2900 Queen Lane, Philadelphia, PA 19129, USA.
E-mail addresses: RR79@drexel.edu (R. Raghupathi), huh@email.chop.edu (J.W. Huh).

https://doi.org/10.1016/j.expneurol.2019.04.004
Received 30 November 2018; Received in revised form 15 March 2019; Accepted 8 April 2019
Available online 10 April 2019
0014-4886/

Berger et al., 2004; Buttram et al., 2007; Newell et al., 2015; Wallisch et al., 2017; Whalen et al., 2000).

Activation of microglia, the resident immuno-competent cells in the brain, is thought to play an important role in the acute and chronic neurodegeneration observed following brain injury (Beynon and Walker, 2012; Graeber and Streit, 2010; Hanisch and Kettenmann, 2007; Kreutzberg, 1996; Nimmerjahn et al., 2005; Ransohoff and Perry, 2009). The role of microglia in acute and chronic neurodegenerative events following pediatric TBI is being defined. We and others have demonstrated that impact trauma to the immature animal resulted in activation of microglia in multiple brain regions exhibiting evidence of neuronal death and axonal injury and have implicated neuroinflammation as one mechanistic basis for spatial learning and working memory deficits (Chhor et al., 2017; Hanlon et al., 2016; Hanlon et al., 2017; Pullela et al., 2006; Simon et al., 2018; Tong et al., 2002; Zhang et al., 2015). Minocycline, an antibiotic with anti-inflammatory properties, has generally been found to be neuroprotective in multiple animal models of adult or toddler-age TBI (Abdel Baki et al., 2010; Homsi et al., 2009; Homsi et al., 2010; Lam et al., 2013; Sangobowale et al., 2018; Simon et al., 2018; Siopi et al., 2012; Siopi et al., 2011). In contrast, administration of minocycline to the brain-injured neonate rodents reduced microglial proliferation but did not reverse cell death or attenuate spatial learning deficits (Chhor et al., 2017; Hanlon et al., 2016; Hanlon et al., 2017) suggestive of a differential age-at-injury response to treatment.

To evaluate a direct role for microglia activation following pediatric TBI, the present study utilized clodronate (dichloromethylene-bisphosphonate, Cl2MBP) to deplete resident microglia immediately after trauma. Liposome-packaged clodronate is taken up by and induces the apoptosis of phagocytes (Lehenkari et al., 2002; van Rooijen and van Kesteren-Hendrikx, 2003) and has been successful in significantly decreasing microglia numbers in the brain (Asai et al., 2015; Drabek et al., 2012; Faustino et al., 2011; Kumamaru et al., 2012). The hypothesis to be tested in the current study was that by directly removing the resident brain microglia in a clinically-relevant model of pediatric TBI will reduce neuronal and axonal degeneration leading to an attenuation of both functional and behavioral deficits.

2. Methods

2.1. Traumatic brain injury

All surgical procedures were done in accordance with the rules and regulations of the Institutional Animal Care and Use Committee at Drexel University College of Medicine. On postnatal day 11, male and female Sprague-Dawley rat pups (Charles River Laboratories, Wilmington MA) were randomly assigned to either receive a closed head injury ($N = 53$) or treated as sham-injured controls ($N = 45$) as previously described (Hanlon et al., 2017; Raghupathi and Huh, 2007). Animals were anesthetized using isoflurane (Patterson Veterinary, Greeley CO, 5% induction, 2–3% maintenance) and a 2 cm incision was made to expose the skull and the periosteum was cleared. At 4 min after the start of anesthesia, animals were placed in plastic rodent restrainer (Braintree Scientific, Braintree MA), and moved to the stage of the electronic controlled cortical impact device (eCCI, Custom Design and Fabrication, Richmond VA). The piston tip (5 mm silicone impactor tip) was zeroed over the left parietal cortex midway between the bregma and lambda sutures, the anesthesia was stopped and when the animal reacted to a tail pinch, the impactor was electrically driven 3 mm into the intact skull at velocity of 5 m/s (dwell time of 100 ms). Following impact, animals were placed on their backs, the times to normal breathing (apnea) and right themselves (righting reflex) were recorded. Sham-injured animals were anesthetized and surgically prepared but did not receive an impact; following surgery, anesthesia was removed, and righting reflex was determined. Once animals righted themselves, they were re-anesthetized and the scalp was sutured shut. Animals recovered in a separate cage for at least 30 min before being placed back with the dam. Surgical procedures and recovery occurred on heating pads at 37 °C to maintain the body temperature.

2.2. Clodronate administration

At 24 h after surgery/injury, sham- and brain-injured animals were randomly assigned to receive intracerebral injections of liposome-encapsulated clodronate (Clodrosome® 5 mg/ml, $N = 23$ sham-injured and 25 brain-injured) or empty liposomes containing phosphate-buffered saline (Encapsome®, $N = 22$ sham-injured and 23 brain-injured). Animals were anesthetized with isoflurane (5% induction, 1–2% maintenance), sutures were removed, the incision site was reopened, the skull was cleaned, and the animals were placed in a stereotactic head holder. A burr hole was drilled in the skull and a 10 µL Hamilton® 80,000 1701 N syringe was used to inject 10 µl of the liposomal suspension (liposome size = 2 µm, Encapsula NanoSciences, Brentwood TN) into the cortex (coordinates: −1.5 mm anterior-posterior (AP), 1.7 mm medial-lateral (ML) and 1.7 mm dorsal-ventral (DV)) and the thalamus (coordinates: −3.5 mm AP, 1.7 mm ML and 3.5 mm DV) (Paxinos and Watson 3rd edition) at a rate of 1 µl/min. Following surgery, animals recovered in a separate cage for at least 60 min before being placed back with the dam. Surgical procedures and recovery occurred on heating pads at 37 °C to maintain the body temperature.

2.3. Histology and immunohistochemistry

Animals were euthanized with sodium pentobarbital (390 mg/Kg, Euthasol® and Virbac, Fort Worth TX) and transcardially perfused with 10% formalin. Brains were removed and processed for histology and immunohistochemistry as previously described (Hanlon et al., 2016; Hanlon et al., 2017). Sections (40 µm thick, 500 µm apart) between +1 and -6 mm relative to Bregma were mounted on gelatin-coated slides and stained for Fluoro-Jade B (FJB) or Nissl-myelin (2% Cresyl Violet and 0.2% Cyanine R) (Hanlon et al., 2016). Additional sets of sections were evaluated for microglia using antibodies for anti-ionized calcium-binding adaptor molecule 1 (Iba1, Wako, Richmond VA, 1:20,000, cat 019-19741) and CD68 (Clone ED1, BioRad/AbD Serotech, Hercules CA, 1:500, cat # MCA341), and traumatic axonal injury using a polyclonal antibody to the C-terminal end of amyloid precursor protein (APP, Zymed, San Francisco CA, 1:2000, cat # PA1-84165). For anti-APP immunohistochemistry, antigen retrieval was executed by incubation with 10 mM sodium citrate (pH 6.5) in a 60 °C water bath for 20 min. Primary antibody binding was detected using biotinylated donkey anti-rabbit IgG (Jackson ImmunoResearch, West Grove PA, 1:1000 for APP and 1:500 for Iba1, cat # 711-065-152) or biotinylated donkey anti-mouse IgG (Jackson ImmunoResearch, West Grove PA, 1:500 for ED-1, cat # 715-065-151). Antibody binding was visualized using the ABC Elite System with diaminobenzidine (Vector Laboratories, Burlingame CA, cat # SK-4100).

Quantification in the cortex (layers 2 through 5 of the retrosplenial, motor and somatosensory cortices), hippocampus (dorsal subiculum) and thalamus (dorsolateral and lateral geniculate nuclei), and was conducted by counting labeled profiles (Iba1, ED-1, FJB) in 3–5 high power field (HPF) images (20× magnification) per section across 3–5 non-adjacent sections. ED-1(+) profiles were counted as separate phenotypes: amoeboid morphology (enlarged, rounded cells with few to no visible processes) and rod morphology (elongated cells with thick cell bodies and few to no visible processes). Counts of Iba1(+) profiles at the 15- and 35-day time points were based on the presence of a discernable cell body with elongated processes (resting) or an amoeboid appearance with no processes (activated); Iba1(+) cells were not counted at 3 days post-injury because in brains injected with empty liposomes the Iba-1 staining was very dense and precluded the ability to identify individual cells while all Iba-1(+) cells were depleted by clodronate. Amyloid precursor protein-labeled and FJB(+) profiles were

quantified in the white matter and thalamus over 3–5 coronal sections as previously described (DiLeonardi et al., 2009; Hanlon et al., 2016; Hanlon et al., 2017). The extent of tissue loss within the cortex and thalamus was quantified over 3–5 Nissl-myelin stained coronal sections as previously described (Raghupathi and Huh, 2007); the intensity of staining was not a factor in outlining the areas to be measured into account. Data collection and analysis were performed by LAH and JWH who were blinded to the injury and treatment status of the samples.

2.4. Cortical evoked field potential

Animals were anesthetized with 5% isoflurane, decapitated, and the brain was rapidly removed and placed in oxygenated (95% oxygen/5% carbon dioxide) ice-cold artificial cerebrospinal fluid (aCSF) containing the following (in mM): sodium chloride 130, sodium bicarbonate 24, glucose 10, potassium chloride 3.5, sodium biphosphate 1.25, magnesium sulfate 1.5, calcium chloride 2). Coronal slices (450 μm thick) at 1–1.2 mm anterior (containing the forelimb motor cortex) and 3–3.5 mm posterior (containing the hindlimb motor cortex) to bregma were obtained using a Vibratome® (1000 Plus, St Louis MO). Slices were incubated in aCSF for 30 min at 37 °C and 30 min at room temperature and placed in a recording chamber where they were continuously bathed with fresh aCSF for the duration of recording. A bipolar, tungsten stimulating electrode (World Precision Instruments, Sarasota FL) was placed in layer 2 of the forelimb or hindlimb motor cortex and a pulled glass recording pipette filled with aCSF was placed in layer 5 of the same cortex (offset by approximately 300 μm from the stimulating electrode). Potentials were evoked using constant current pulses (200 μs duration) from a Master-8 pulse stimulator (A.M.P·I, Jerusalem Israel) at increasing intensities (manual current stepping from 0 to 1000 μA) and recorded using an Axoclamp 2B amplifier. Slices from sham- and brain-injured animals reacted similarly to current input and demonstrated a plateau around 800 μA, therefore all data were quantified at this current as the average of 5 sweeps. The amplitude of the signal was measured as the difference (in millivolts) between baseline and the middle of the primary peak and the latency of the signal was measured as the difference in time (in milliseconds) between the beginning of the stimulus artifact and the middle of the primary peak. All quantification was performed by LAH and RR who were blinded to the injury and treatment status of each animal.

2.5. Spatial learning and memory

Spatial learning was assessed on days 10–13 and 28–31 in separate groups of animals using the Morris water maze as previously described (Hanlon et al., 2016; Hanlon et al., 2017). Animals were trained over 4 days to find the location of the hidden platform submerged approximately 1 cm below the surface of the water (20 °C) as previously described (Hanlon et al., 2016; Hanlon et al., 2017). Animals were trained to locate the submerged platform over 4 trials on each of 4 days and the latency to find the platform was averaged across trials for each day. On the 5th day (probe trial), the platform was removed from the pool and the swimming pattern of each animal was tracked (AccuScan Instruments Inc., Columbus OH) for two 60-s trials to assess time spent in zones closest to or furthest from the original location of the platform. Following the probe trials, the platform was placed back in the water and the water level was lowered so that the top inch of the platform was exposed, and a flag was adhered to the top of the platform. The latency to locate the visible platform was recorded in one trial. Behavioral assessments were performed by LAH who was blinded to the injury and treatment status of the animals.

2.6. Straight-path swim task

Animals were trained to swim the length of the 48″ aquarium in a straight path as previously described (Stoltz et al., 1999). The water in the tank was maintained at 18–20 °C and a cue rat was placed on the platform and a flag was adhered to the side of the platform to make sure the test rats could see the platform. On the training day, the tank was separated into quarters to form the 4 training release points at varying distances from the platform and animals were released from these points in order until they could swim the length of the tank in a straight path without turning or running into the sides. At 24 h after training, animals were subjected to one acclimation trial released from the furthest point from the platform in order to familiarize them with the task followed by the test trials which were recorded for quantification. Animals were tested by cage and allowed to rest for 2 min between trials. Test trials were terminated when animals completed 3 straight-path runs without turning or running into the walls of the tank. Data is presented as the average number of strokes across 3 runs. Behavioral assessments were performed by LAH who was blinded to the injury and treatment status of the animals.

2.7. Statistical analysis

All statistics were performed using Statistica 7 (StatSoft, Tulsa OK). All data are presented as mean ± standard error of the mean. Data were compared using a 3-way ANOVA (injury status, treatment status, time) or a 2-way ANOVA (injury status, treatment status) as necessary. Spatial learning latencies were compared using a 2-way (injury and treatment status) repeated measures ANOVA (days of training). The percent of tissue loss was compared between the brain-injured groups using the Student's *t*-test. When necessary, post-hoc analyses were performed using the Newman-Keuls test and a value of $p \leq 0.05$ was considered significant. Sex was used as a covariate in all analyses.

3. Results

3.1. Acute neurologic outcomes

Closed head injury to the 11-day-old rat resulted in a linear skull fracture below the impact site that was associated with apnea (9–20s) and a loss of righting reflex (Table 1). Brain-injured animals took a significantly longer time to right themselves after injury compared to sham-injured animals after removal of anesthesia ($F_{(3,72)} = 22.1$, $p < 0.00001$). Five animals died as a result of the impact (10%); collectively, these data are suggestive of a moderate level of trauma. There were no differences in body weights and injury-induced apnea and righting reflex latencies between the groups designated for the different behavioral, histologic and electrophysiologic outcomes (Table 1).

3.2. Clodronate-mediated depletion and repopulation of microglia/macrophages in the sham-injured animals

Injection of empty liposomes into the cortex of sham-injured animals (Fig. 1A-C) resulted in microglia staining with Iba1 that were predominantly in the resting phase as indicated by the small cell bodies and extensive processes at 3 (Fig. 1A), 15 (Fig. 1B) and 35 days post-injection (Fig. 1C). Injection of clodronate led to an almost complete depletion of Iba1(+) microglia at 3 days (Fig. 1D) and was localized to 1-2 mm around the injection site. By 15 days (Fig. 1E) and 35 days post-injection (Fig. 1F), however, labeling in sham-injured animals had returned to normal levels and Iba1 immunoreactivity was indistinguishable from encapsome-injected brains. A similar temporal pattern was observed in the thalamus (data not shown).

3.3. Effect of microglia depletion in the cortex

Sham-injured animals injected with empty liposomes into the cortex demonstrated ED-1(+) microglia along the needle track at 3 days post-injection (Fig. 2A) suggestive of microglial activation; by 15 days this had dissipated (Fig. 2B) and few, if any, active cells were observed at

Table 1
Neurologic outcomes following TBI in the neonate.

Group	Time point (days)	N (F, M)	Weight (g)	Apnea (s)	Righting reflex (s)
Sham Empty	3	3 (1, 2)	23.6 ± 1.3	NA	ND
Sham Clodronate		3 (1, 2)	22.5 ± 1.0	NA	ND
Injured Empty		5 (2, 3)	21.2 ± 0.9	11 ± 4	207 ± 36
Injured Clodronate		6 (1, 5)	19.9 ± 0.5	18 ± 2	196 ± 42
Sham Empty	15	5 (2, 3)	22.7 ± 0.6	NA	56 ± 13
Sham Clodronate		5 (2, 3)	23.6 ± 0.5	NA	59 ± 6
Injured Empty		5 (3, 2)	23.0 ± 0.2	13 ± 2	199 ± 33
Injured Clodronate		5 (2, 3)	23.3 ± 0.5	15 ± 3	163 ± 27
Sham Empty	35	5 (2, 3)	23.6 ± 0.6	NA	72 ± 4
Sham Clodronate		6 (2, 4)	23.3 ± 1.3	NA	69 ± 13
Injured Empty		5 (2, 3)	24.2 ± 0.4	13 ± 1	156 ± 31
Injured Clodronate		5 (2, 3)	24.2 ± 0.9	18 ± 2	191 ± 29
Sham Empty	28	9 (5, 4)	22.8 ± 1.0	NA	107 ± 12
Sham Clodronate		9 (5, 4)	22.1 ± 1.2	NA	101 ± 11
Injured Empty		8 (4, 4)	24.0 ± 0.7	15 ± 1	183 ± 21
Injured Clodronate		9 (4, 5)	22.1 ± 0.9	17 ± 1	230 ± 28

Animals in the 15-day and 35-day survival groups were tested for spatial learning on days 10–14 and 28–32 respectively and euthanized for histology. Animals in the 28-day survival group underwent testing in the straight path swim test on days 26–27 post-injury and euthanized for electrophysiology. Values represent means ± standard error of the mean. NA, not applicable; ND, not determined.

35 days (Fig. 2C). Microglia stained with ED-1 were observed between 1 mm and 6 mm posterior to bregma in brain-injured animals injected with empty liposomes (Fig. 2D-F). At 3 days ED-1(+) cells were observed in all layers of the parietal and occipital cortices (Fig. 2D) and was primarily present in layers 3–5 at 15 (Fig. 2E) and 35 days after injury (Fig. 2F). No ED-1-labeled cells were present in sham-injured animals injected with clodronate at any time point (Fig. 2G-I). A few ED-1(+) cells were observed in clodronate-injected brain-injured animals at 3 days post-injury (Fig. 2J), with more cells 15 (Fig. 2K) and 35 days (Fig. 2L) post-injury. In brain-injured animals, the ED-1-labeled cells appeared as either amoeboid (inset, panel L) or rod-like (inset, panel K). Quantification of amoeboid ED-1-labeled microglia (Fig. 2M) revealed a greater number of cells in brain-injured animals compared to their sham-injured counterparts (injury status, $F_{(1,46)} = 75.8$, $p < 0.0001$) with the highest number at 3 days post-injury (time, $F_{(2,46)} = 8.2$, $p < 0.001$). Based on a significant interaction effect between injury status, time and treatment ($F_{(2,46)} = 9.3$, $p < 0.0005$), post-hoc analyses revealed that at 3 days, more ED-1(+) amoeboid cells were present in empty liposome-injected brain-injured animals compared to those injected with clodrosome ($p < 0.0002$). In contrast at 35 days post-injury, this pattern was reversed wherein clodrosome-injected brains had a greater number of amoeboid microglia compared to those injected with empty liposomes ($p < 0.02$, Fig. 2M). Brain-injured animals exhibited more ED-1(+) rod-like microglia (Fig. 2N, injury status, $F_{(1,46)} = 28.0$, $p < 0.0001$) at 3 days post-injury (time, $F_{(2,46)} = 4.3$, $p < 0.02$) but there was no significant effect of injury status, time and treatment. Sex of the animal did not affect counts of either amoeboid ($F_{(2,46)} = 0.2$, $p = 0.98$) or rod ($F_{(2,46)} = 0.8$, $p = 0.57$) microglia. Quantitative analysis of Iba-1 immunoreactive cells within the cortex at the 15- and 35-day time points revealed that brain-injured animals exhibited more reactive microglia compared to sham-injured animals (Fig. 2O, injury status, $F_{(1,34)} = 303.5$, $p < 0.00001$). Based on a significant interaction effect between injury status, time and treatment ($F_{(1,34)} = 49.3$, $p < 0.0001$), post-hoc analyses revealed that at 15 days post-injury, clodrosome-injected, brain-injured rats contained fewer active Iba-1(+) microglia compared to the brain-injured rats injected with empty liposomes (Fig. 2O, $p < 0.0002$); at 35 days, similar numbers of Iba-1(+) active microglia

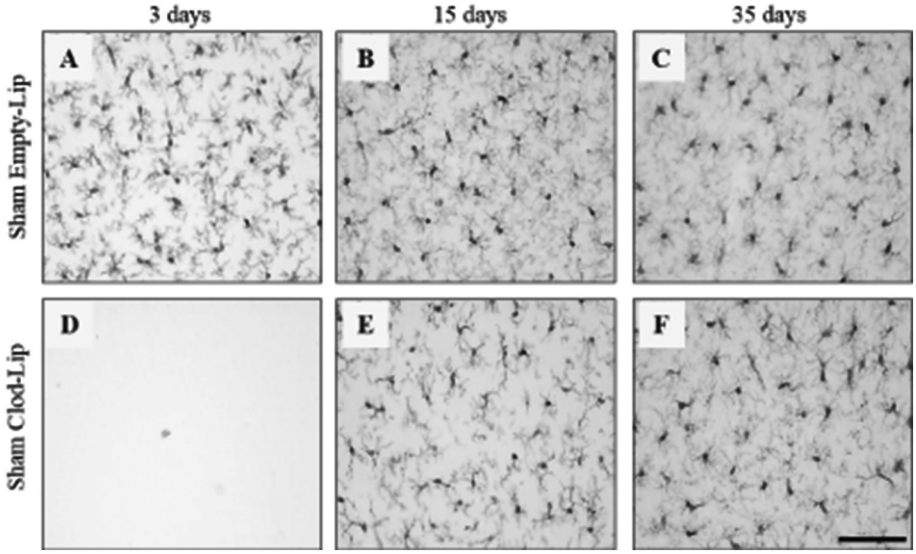

Fig. 1. Iba-1(+) microglia in the cortex following clodronate-induced depletion.
Representative photomicrographs of sham-injured animals injected with empty liposomes (A-C) or clodronate liposomes (D-F) at 3 (A,D), 15 (B,E), and 35 (C,F) days post-injury. Scale bar in panel L = 100 μm for all panels.

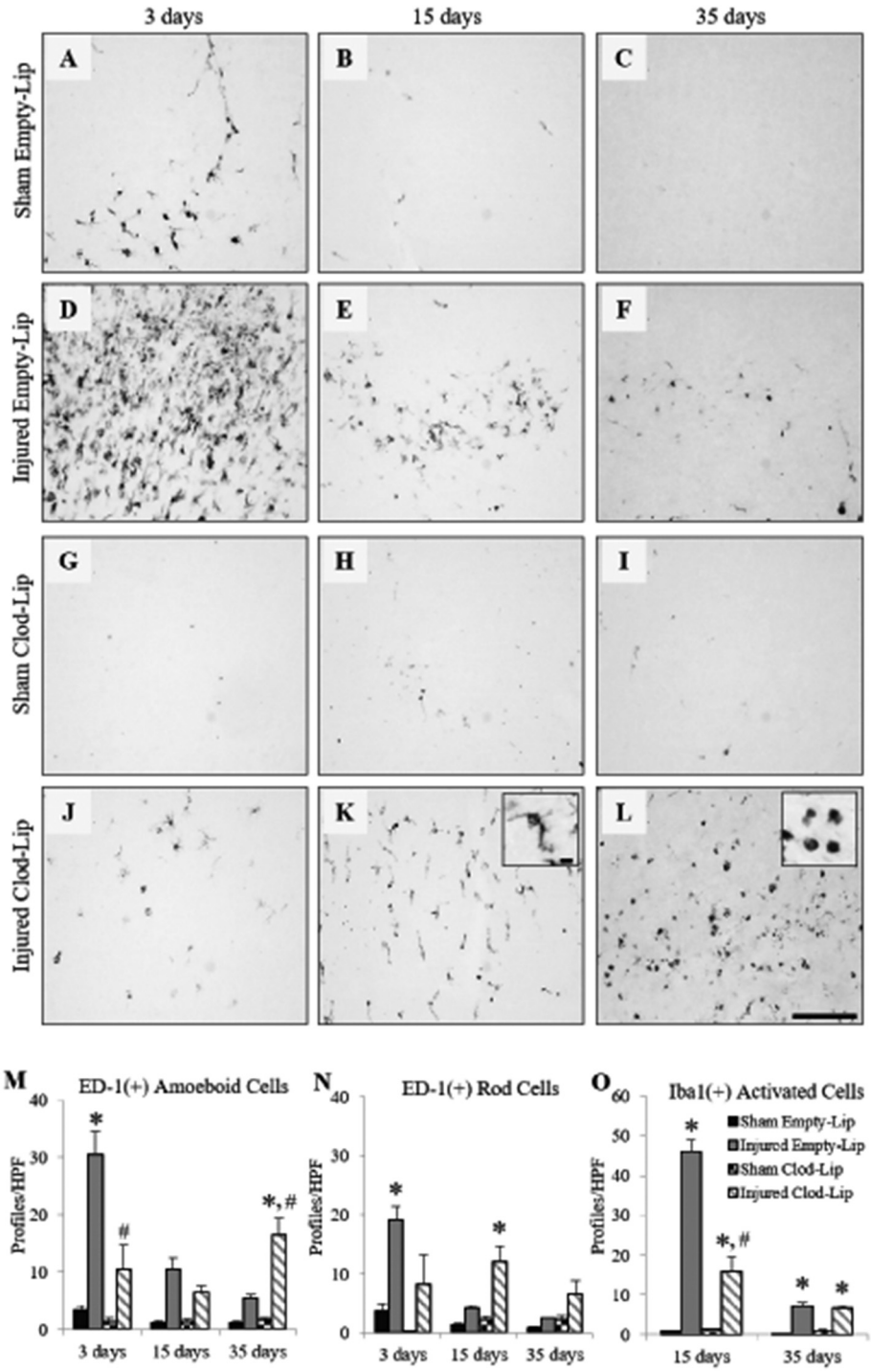

Fig. 2. Microglia activation in the cortex following clodronate-induced depletion.
Representative photomicrographs of ED-1 immunoreactivity in sham- (A-C) and brain-injured (D-F) animals injected with empty liposomes and sham- (G-I) and brain-injured (J-L) animals injected with clodronate liposomes at 3 (A,D,G,J), 15 (B,E,H,K), and 35 (C,F,I,L) days post-injury. Inset in Fig. K shows a representative photomicrograph of a rod microglia/macrophage characterized by an elongated, thick cell body and short processes. Inset in Fig. L shows a representative photomicrograph of an amoeboid microglia characterized by a round cell body and few, if any, visible processes. Quantification of ED-1(+) microglia exhibiting amoeboid (M) and rod (N) morphologies. Quantification of Iba-1(+) cells exhibiting activated morphology as described in Methods (O). Bar graphs represent group means and error bars represent the standard error of the mean. *, $p \leq 0.05$ compared to time-matched sham-injured group; #, $p \leq 0.05$ compared to time-matched brain-injured empty liposome-injected animals. Scale bar in L = 100 μm for all panels; scale bar within the inset in panel K = 10 μm for both inset micrographs.

were observed in both empty liposome- and clodrosome-injected rats (Fig. 2O, $p = 0.79$). Sex of the animal did not affect counts of Iba-1-labeled cells ($F_{(1.26)} = 0.91$, $p = 0.35$).

A few FJB(+) cells were visible along the injection track of sham-injured animals at 3 days post-injury (Fig. 3A and G) which dissipated over time (Fig. 3B,C,H,I). Brain injury led to the appearance of degenerating cells in the cortex in both empty liposome- (Fig. 3D-F) and clodronate-injected animals (Fig. 3J-L). Degenerating cells were primarily observed in layers 2–5 of the parietal and occipital cortices between 1 mm and 6 mm posterior to bregma at all times post-injury, with a greater extent in animals injected with clodronate. Quantification revealed a greater number of cells in brain-injured compared to sham-injured animals (injury status, $F_{(1,46)} = 93.1$, $p < 0.0001$, Fig. 3M) and a greater number in brain-injured animals injected with clodronate (injury status x treatment, $F_{(1,46)} = 20.9$, $p < 0.0001$). The sex of the animals did not affect injury- or treatment-induced neurodegeneration (injury status x treatment x sex, $F_{(2,46)} = 0.6$, $p = 0.76$). The increase in neurodegeneration at 15 days post-injury did not affect the injury-induced reduction in cortical area in either encapsome- (8.4 ± 0.6%) or clodrosome-injected- (5.6 ± 1.6%, $t = -1.6$, $p = 0.15$) animals.

To determine the functional consequence of increased number of FJB(+) cells in the parietal and occipital cortices, extracellular evoked potentials were recorded at 28 days post-injury in layer 5 of the hindlimb region of the parietal cortex (3–3.5 mm posterior to bregma) following stimulation of layers 2–3. The evoked potentials in sham-injured animals injected with either empty or clodronate-filled liposomes

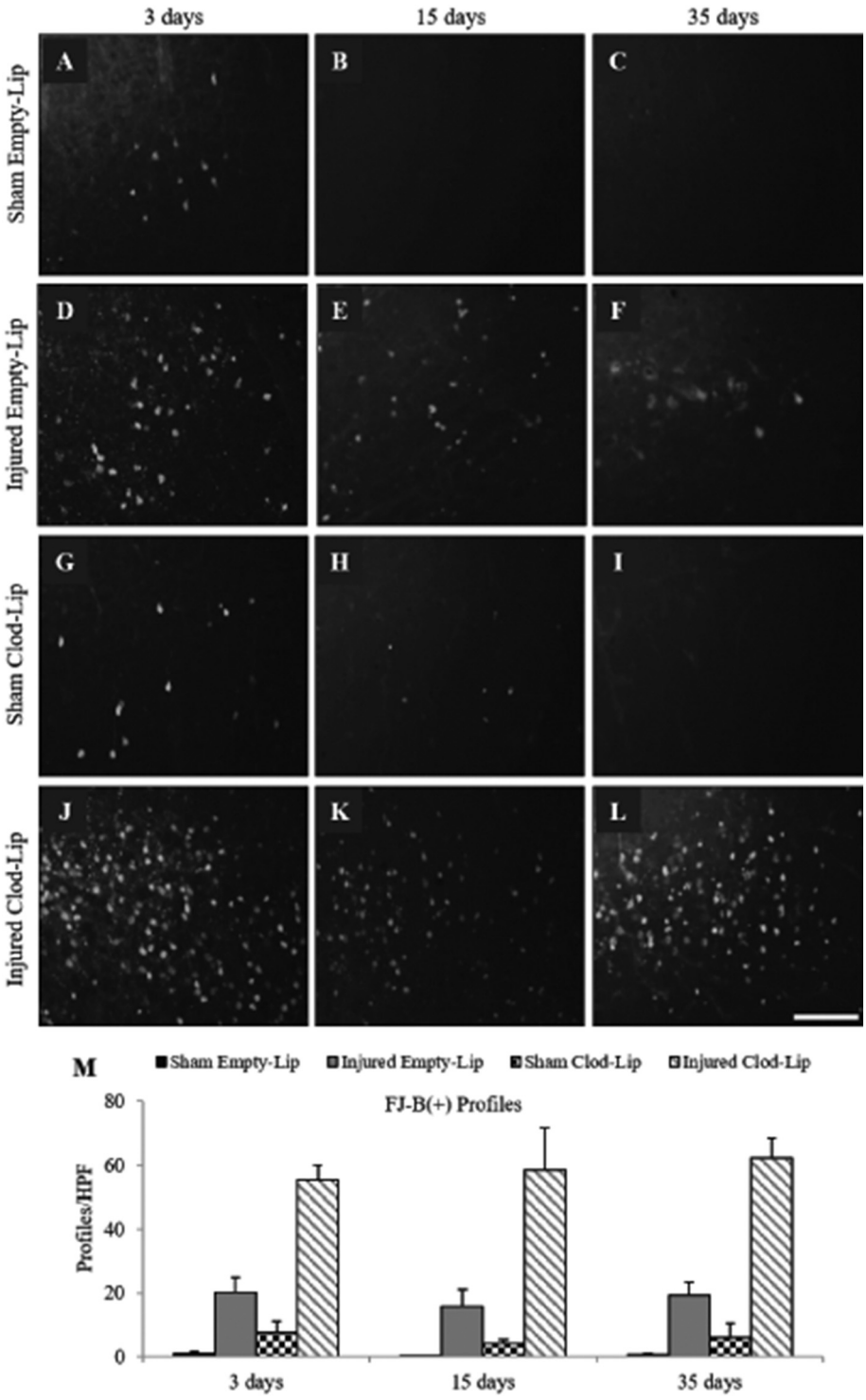

Fig. 3. Neurodegeneration in the cortex following clodronate-induced microglia depletion.
Representative photomicrographs of FJB-labeling in sham-injured (A-C) and brain-injured (D-F) animals injected with empty liposomes and sham-injured (G-I) and brain-injured (J-L) animals injected with clodronate liposomes at 3 (A,D,G,J), 15 (B,E,H,K), and 35 (C,F,I,L) days post-injury. (M) Quantification of FJB(+) profiles. Multivariate analysis of variance revealed that injury status, irrespective of treatment and time, was significant ($p < 0.0001$), and interaction between injury and treatment was significant at all time points ($p < 0.0001$); detailed statistical descriptions are provided in the Results. Bar graphs represent group means and error bars represent the standard error of the mean. Scale bar in L = 100 μm for all panels.

were not different from each other (Fig. 4A) suggesting that the repopulation of the microglia over the 4-week post-injection period conferred normalcy to the circuit within the cortex. Similarly, brain-injured animals that received injections of empty liposomes exhibited a normal evoked signal albeit with a shorter latency (Fig. 4A). In contrast, the amplitude of the signal in clodronate-injected brain-injured animals was larger than that observed in corresponding sham-injured animals although the latencies were similar (Fig. 4A). A 2-way ANOVA on the amplitudes revealed a significant group effect ($F_{(3,24)} = 3.5$, $p < 0.05$, Fig. 4B) and the post-hoc analysis confirmed that the amplitude of the signals from brain-injured clodronate-injected animals were significantly larger than those from either the corresponding sham-injured group ($p < 0.05$) or brain-injured empty liposome injected animals ($p < 0.05$). Analysis of the latency of the deflection of signals showed a significant group effect ($F_{(3,24)} = 4.71$, $p < 0.05$, data not shown) with the post-hoc analysis indicating that signals from brain-injured animals injected with the empty liposomes were faster than the signals from the corresponding sham-injured animals ($p < 0.02$). There were no differences in any measure between the sexes (amplitude: $F_{(3,24)} = 0.4$, $p = 0.76$; latency: $F_{(3,24)} = 1.2$, $p = 0.32$).

To evaluate whether alterations in the activity of local cortical circuits in the hindlimb region of the motor cortex were specifically

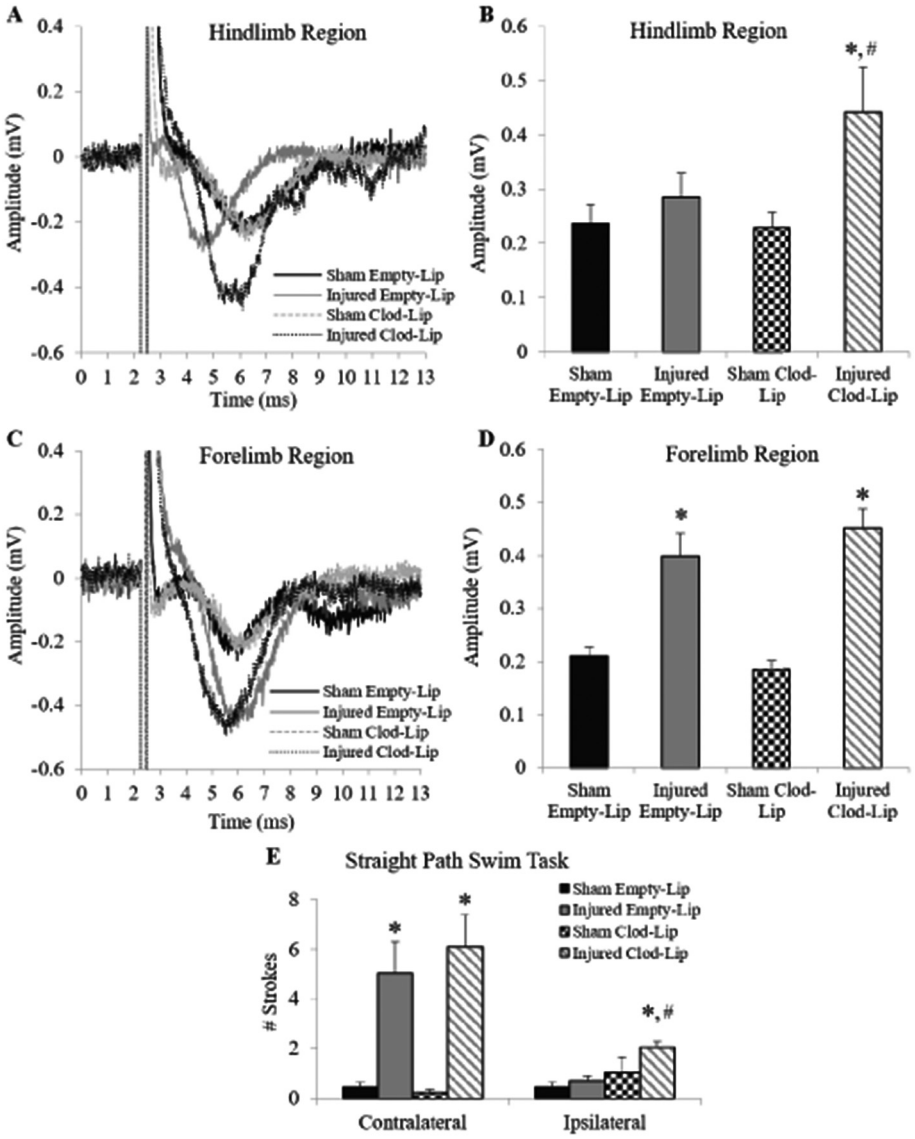

Fig. 4. Extracellular evoked potentials in the cortex at 4 weeks following clodronate-induced microglia depletion.
Representative traces from the hindlimb region (A) and forelimb region (C) of the motor cortex of sham-injured and brain-injured animals that received either empty or clodronate liposomes. (B, D) Quantification of the amplitude of the maximum deflection of the traces from the respective regions. (E) Forelimb motor deficits in the straight path swim task. Bar graphs represent group means and error bars represent the standard error of the mean. *, $p \leq 0.05$ compared to corresponding sham-injured group; #, $p \leq 0.05$ compared to corresponding brain-injured animals injected with empty liposomes.

related to presence of neurodegeneration and activated microglia, evoked neuronal activity was recorded from the forelimb region of the motor cortex at 1–1.2 mm anterior to bregma, a region that does not demonstrate evidence of FJB reactivity or ED-1 immunoreactivity (data not shown). Interestingly, qualitative evaluation of the traces revealed that the amplitudes of the signal from brain-injured animals were larger compared to sham-injured animals irrespective of treatment (Fig. 4C) suggestive of an increase in excitability of this local circuit. Quantitative analyses of amplitudes revealed a significant group effect ($F_{(3,25)} = 17.5$; $p < 0.001$) which was independent of sex ($F_{(3,25)} = 0.2$; $p = 0.93$). The post-hoc analysis indicated that brain-injured animals that received either empty or clodronate liposomes had significantly larger signals than the corresponding sham-injured animals ($p < 0.001$, Fig. 4D). However, there was no significant effect of either group ($F_{(3,25)} = 0.5$; $p = 0.69$) or sex ($F_{(3,25)} = 0.8$; $p = 0.50$) on the latency to the deflection of the signal (data not shown). The observed increase in excitability in the forelimb cortical region of brain-injured animals may occur due to disinhibition in the local circuit which can be behaviorally evaluated (Stoltz et al., 1999). Although sham- and brain-injured animals were able to swim the straight path with similar latencies (data not shown), the right front paw of brain-injured animals (contralateral to the site of impact) was used to a greater extent compared to the sham-injured cohort ($F_{(3,27)} = 11.1$; $p < 0.001$, Fig. 4E) but was not dependent on sex ($F_{(3,27)} = 0.4$; $p = 0.74$). The number of strokes with the contralateral forelimb, however, did not differ between brain-injured animals that were injected with empty liposomes and those were injected with clodronate liposome ($p = 0.41$). Brain-injured animals injected with empty liposomes exhibited normal use of the forepaw ipsilateral to the impact whereas those that were injected with clodronate liposomes had a modest increase in their use of this limb ($F_{(3,27)} = 3.9$; $p < 0.05$, Fig. 4E).

3.4. Effect of microglia depletion in lateral white matter tracts

Because liposomes were injected into the deeper layers of the cortex (1.7 mm from the dural surface), the underlying white matter may be affected by diffusion of the liposomes. Injected of clodronate in sham- (Fig. 5C) or brain-injured animals (Fig. 5D) depleted microglia in the corpus callosum, cingulum, and lateral white matter at the 3-day time point compared to animals injected with empty liposomes (Fig. 5A and B). A few APP-labeled axons were observed in sham-injured animals likely due to the intracerebral injection (Fig. 5E and G) whereas brain-injured animals demonstrated robust APP labeling (Fig. 5F and H). Brain-injured animals had significantly more APP labeling compared to sham-injured animals regardless of whether they were injected with

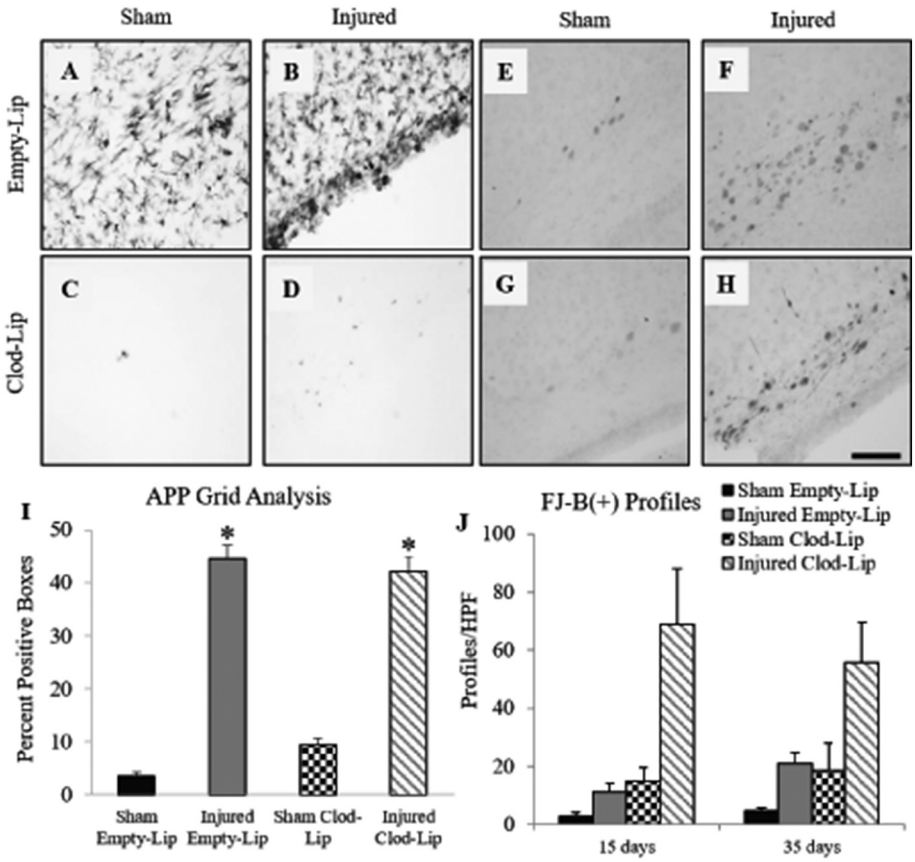

Fig. 5. Pathologic alterations in the white matter following clodronate-induced microglia depletion. Representative photomicrographs of Iba-1(+) microglia at 3 days post-injury in the white matter tracts below the impact site of sham- (A) and brain-injured (B) animals injected with empty liposomes and sham- (C) and brain-injured (D) animals injected with clodronate liposomes. Representative photomicrographs of APP(+) profiles at 3 days post-injury in sham- (E) and brain-injured (F) animals injected with empty liposomes and sham- (G) and brain-injured (H) animals injected with clodronate liposomes. (I) Quantification of the extent of APP labeling using the grid analysis described in the methods. (J) Quantification of FJB(+) profiles. Bar graphs represent group means and error bars represent the standard error of the mean. *, $p \leq 0.05$ compared to corresponding sham-injured group. Scale bar in panel H = 100 μm for all panels.

empty or clodronate liposomes ($F_{(3,14)} = 59.6$, $p < 0.001$, Fig. 5I) Whereas depletion of microglia did not affect axonal injury, the number of FJB(+) profiles were significantly higher at both 15 and 35 days post-injury in the animals that were injected with clodronate ($F_{(3,25)} = 14.7$, $p < 0.001$, Fig. 5J). There was no effect of sex ($F_{(3,25)} = 0.60$, $p = 0.62$).

3.5. Effect of microglia depletion in the thalamus

As observed in the cortex, brain injury resulted in activation of ED-1(+) microglia in multiple thalamic nuclei (laterodorsal ventrolateral, posterior, ventral posteromedial) which appeared as amoeboid (injury status effect, $F_{(1,46)} = 126.6$, $p < 0.0000$, Fig. 6A) or rod-like (injury status effect, $F_{(1,46)} = 46.2$, $p < 0.0000$, Fig. 6B) in morphology in the thalamus. Clodronate injection into the thalamus effectively reduced ED-1(+) microglia in both sham- and brain-injured animals at the 3-day time point (Fig. 6A and B). A significant interaction effect between injury status, treatment and time was evident for both amoeboid ($F_{(2,46)} = 13.2$, $p < 0.0001$, Fig. 6A) and rod-like ED-1(+) microglia ($F_{(2,46)} = 3.2$, $p < 0.05$, Fig. 6B). Post-hoc analysis revealed that brain-injured empty-liposome animals had significantly more ED-1(+) amoeboid microglia at 3 ($p < 0.0002$) and 15 days ($p < 0.00002$) post-injury (Fig. 6A) and significantly more ED-1(+) rod-like microglia at 3 ($p < 0.0002$) and 15 days ($p < 0.01$) post-injury (Fig. 6B).Whereas at 3 days empty liposome injected brain-injured animals contained more ED-1(+) amoeboid ($p < .0002$, Fig. 6A) and rod-like microglia ($p < 0.0002$, Fig. 6A) compared to the clodronate-injected cohort, at 35 days the clodronate-injected animals contained a significantly greater number of ED-1(+) amoeboid microglia compared to the empty liposome-injected group ($p < 0.01$, Fig. 6A). There was no effect of sex on ED-1(+) amoeboid ($F_{(6,34)} = 0.5$, $p = 0.84$) or rod microglia ($F_{(6,34)} = 0.2$, $p = 0.99$). Quantitative analysis of Iba-1 immunoreactive cells within the thalamus at the 15- and 35-day time points revealed that brain-injured animals exhibited more reactive microglia compared to sham-injured animals (Fig. 6C, injury status, $F_{(1,34)} = 187.1$, $p < 0.00001$). Based on a significant interaction effect between injury status, time and treatment ($F_{(1,34)} = 21.8$, $p < .00005$), post-hoc analyses revealed that at 15 days post-injury, clodrosome-injected, brain-injured rats contained fewer active Iba-1(+) microglia compared to the brain-injured rats injected with empty liposomes (Fig. 6C, $p < 0.0002$); at 35 days, similar numbers of Iba-1(+) active microglia were observed in both empty liposome- and clodrosome-injected rats (Fig. 6C, $p = 0.06$). Sex of the animal did not affect counts of Iba-1-labeled cells ($F_{(1.26)} = 0.20$, $p = 0.65$). Despite the decrease in ED-1(+) activated microglia in the clodronate-injected animals at 3 days post-injury, there was no difference in the burden of axonal injury (injury status X treatment $F_{(1,14)} = 0.04$, $p = 0.84$, Fig. 6E). However, FJB labeling at all times post-injury was significantly increased in brain-injured animals injected with clodronate liposomes (injury status X treatment, $F_{(1,48)} = 36.1$, $p < 0.0000$, Fig. 6D); there was no effect of sex on FJB reactivity ($F_{(6,35)} = 1.5$, $p = 0.22$). Despite this observation of increased neurodegeneration at the 15-day time point, the injury-induced decrease in area of the thalamus was not different between the animals injected with empty liposomes (14.9 ± 1.5%) and those injected with clodrosome (13.3 ± 1.9%, $t = -0.65$, $p = 0.54$).

3.6. Effect of microglia depletion in the subiculum

Although the hippocampus was not directly targeted, depletion of microglia was observed in the dorsal aspect of the subiculum presumably as a result of diffusion of the liposomes from the thalamic injections. Brain-injured animals had a significantly greater number of ED-1(+) amoeboid (Fig. 7A, $F_{(1,45)} = 29.1$, $p < 0.0000$) and rod-like microglia (Fig. 7B, $F_{(1,45)} = 31.4$, $p < 0.0000$). Based on a significant interaction effect between injury, treatment and time ($F_{(2,45)} = 3.3$,

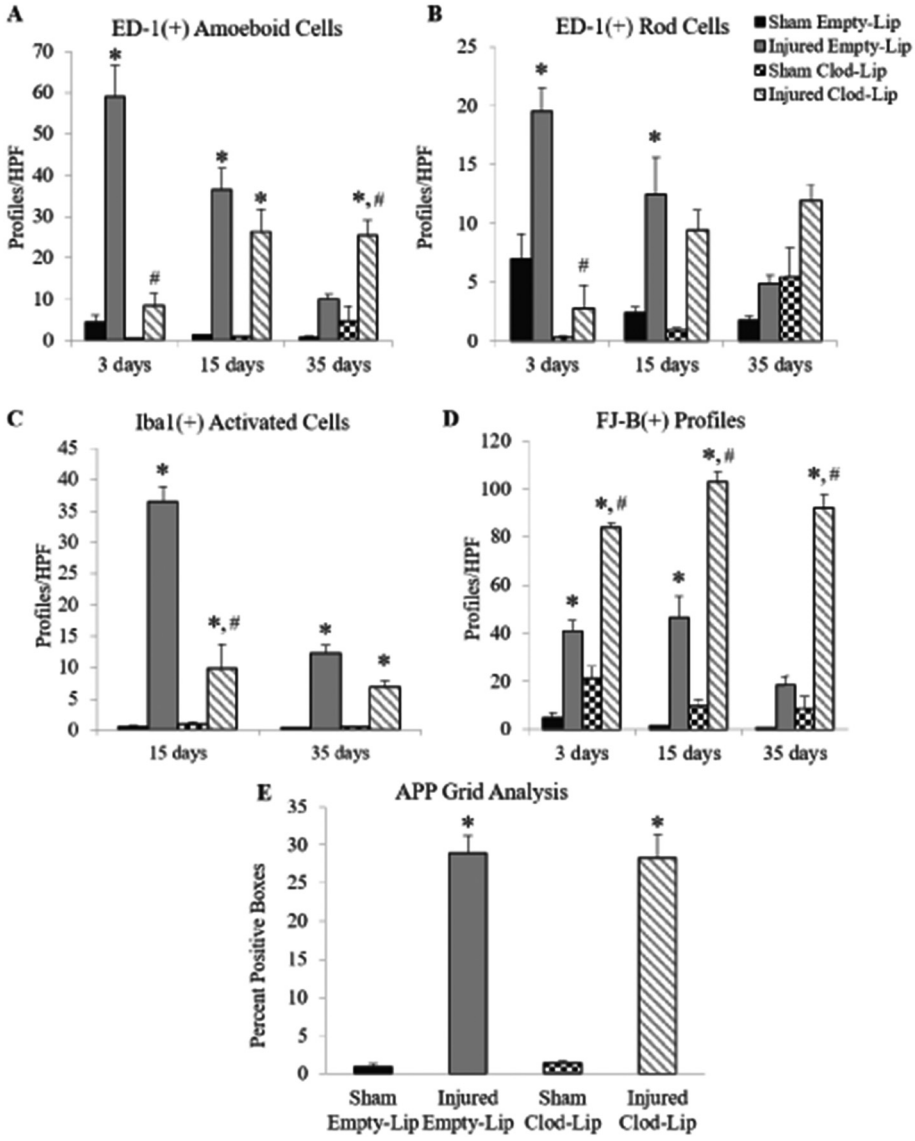

Fig. 6. Pathologic alterations in the thalamus following clodronate-induced microglia depletion.
Quantification of ED-1(+) microglia that exhibit amoeboid (A) or rod (B) morphologies, Iba-1(+) cells exhibiting activated morphology as described in Methods (C), and (D) FJB(+) profiles at 3, 15 and 35 days post-injury. (E) Quantification of APP(+) profiles at 3 days post-injury. Bar graphs represent group means and error bars represent the standard error of the mean. *, $p \leq 0.05$ compared to time-matched sham-injured group; #, $p \leq 0.05$ compared to time-matched brain-injured animals injected with empty liposomes.

$p < 0.05$), a post-hoc analysis revealed that at 35 days, brain-injured animals injected with clodronate had more ED-1(+) amoeboid microglia compared to the empty liposome cohort ($p < 0.02$, Fig. 7A). Interestingly, brain-injured clodronate-injected female rats had significantly more ED-1(+) amoeboid microglia at 35 days post-injury compared to the corresponding male cohort ($p < 0.05$). There was no effect of sex on ED-1(+) rod microglia/macrophages ($F_{6,33} = 0.3$, $p = 0.93$). Quantitative analysis of Iba-1 immunoreactive cells within the subiculum at the 15- and 35-day time points revealed that brain-injured animals exhibited more reactive microglia compared to sham-injured animals (Fig. 7C, injury status, $F_{(1,34)} = 79.7$, $p < 0.00001$). Based on a significant interaction effect between injury status, time and treatment ($F_{(1,34)} = 10.0$, $p < 0.005$), post-hoc analyses revealed that at 15 days post-injury, clodrosome-injected, brain-injured rats contained fewer active Iba-1(+) microglia compared to the brain-injured rats injected with empty liposomes (Fig. 7C, $p < 0.0002$); at 35 days, similar numbers of Iba-1(+) active microglia were observed in both empty liposome- and clodrosome-injected rats (Fig. 7C, $p = 0.81$). Sex of the animal did not affect counts of Iba-1-labeled cells ($F_{(1.26)} = 0.04$, $p = 0.84$). As in the cortex and thalamus, FJB reactivity was increased in the subiculum of brain-injured animals ($F_{(1,48)} = 15.9$, $p < 0.0002$, Fig. 7D). Moreover, brain-injured animals that were injected with clodronate also exhibited more FJB(+) profiles compared to the cohort that were injected with empty liposomes ($F_{(1,48)} = 5.1$, $p < 0.03$, Fig. 7D). There was no effect of sex on FJB reactivity in the subiculum ($F_{3,36} = 0.95$, $p = 0.47$).

Spatial learning and memory were assessed in separate groups of animals on post-injury days 10–14 (Fig. 8A and B) and 28–32 (Fig. 8C and D). On days 10–14, sham-injured animals that were injected with the empty liposomes were able to learn the task in a pattern similar to our earlier observations (Raghupathi and Huh, 2007). Interestingly, intracerebral injections of clodronate into either sham- or brain-injured animals impaired their ability to learn the location of the platform (Fig. 8A) such that there was no significant effect of injury ($F_{(1,51)} = 2.2$, $p = 0.15$) or treatment ($F_{(1,51)} = 2.7$, $p = 0.12$) on spatial learning. In the probe trial, brain-injured animals did, however, spend

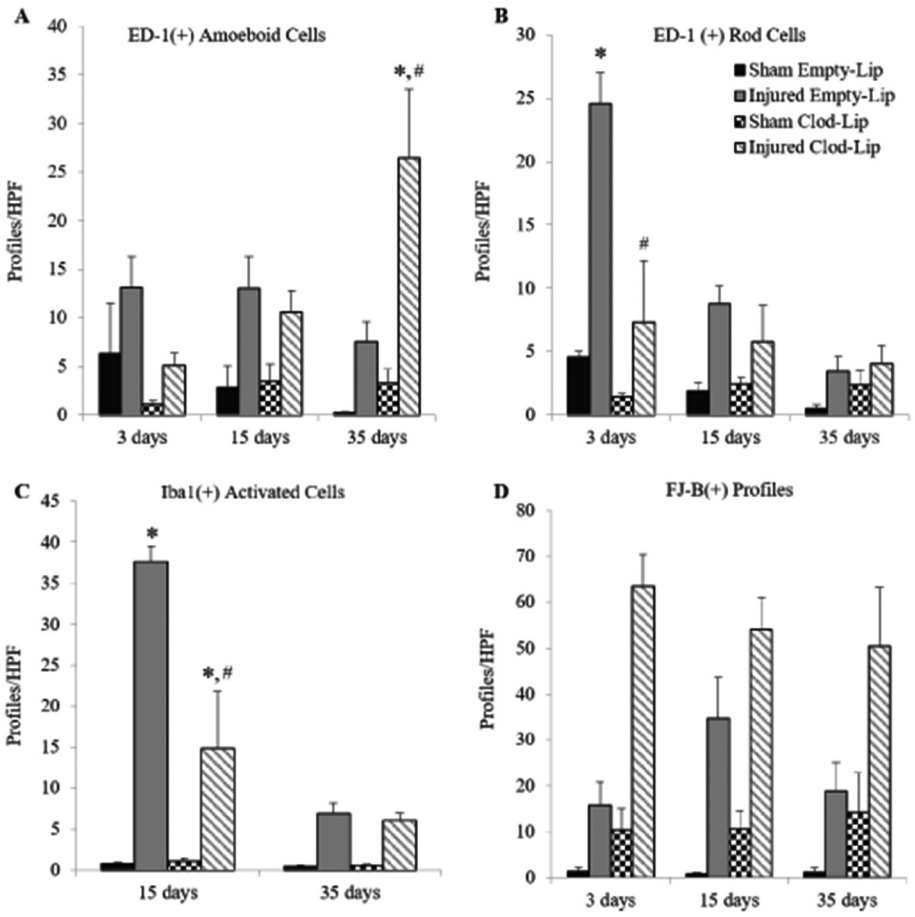

Fig. 7. Pathologic alterations in the dorsal subiculum following clodronate-induced microglia depletion.
Quantification of ED-1(+) microglia that exhibit amoeboid (A) or rod (B) morphologies, (C) Iba-1(+) cells exhibiting activated morphology as described in Methods, and (D) FJB(+) profiles at 3, 15, and 35 days post-injury. Bar graphs represent group means and error bars represent the standard error of the mean. *, $p \leq 0.05$ compared to time-matched sham-injured group; #, $p \leq 0.05$ compared to time-matched brain-injured injected with empty liposomes.

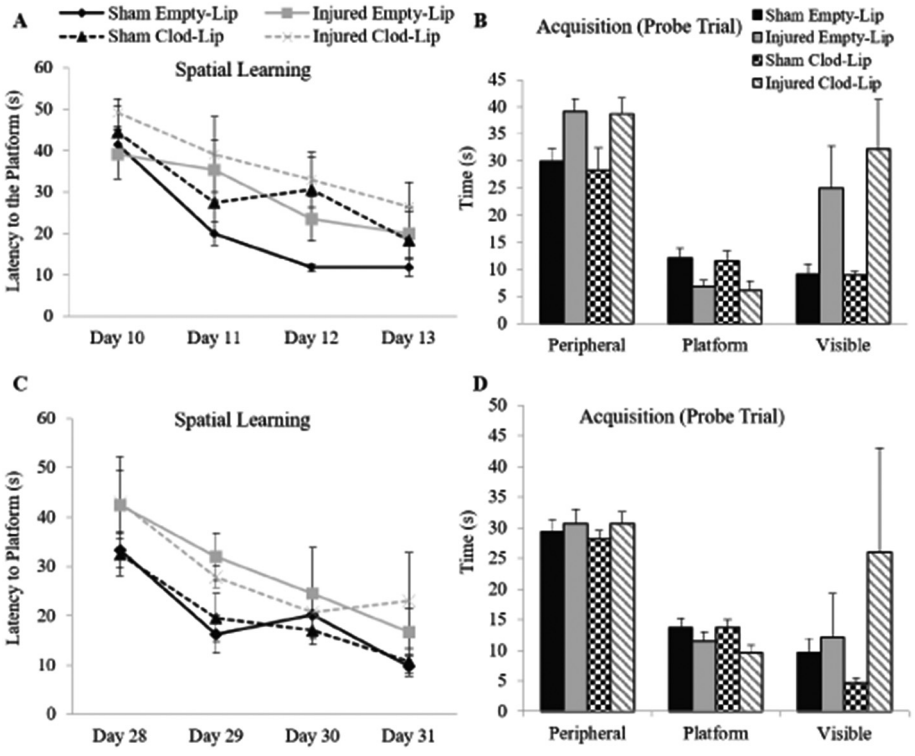

Fig. 8. Spatial learning and memory assessment following clodronate-induced microglia depletion.
Assessment of spatial learning in the Morris water maze presented as latency to find the hidden platform on days 10–13 post-injury (A) and days 28–31 post-injury (C). Probe trial performance on day 14 (B) and day 32 post-injury (D). Bar graphs represent group means and error bars represent the standard error of the mean.

significantly less time in the platform zone compared to sham-injured animals (Fig. 8B, $F_{(1,17)} = 4.7$, $p < 0.05$) although there was no significant effect of injury in the visible platform trial (Fig. 8B, $F_{(1,17)} = 4.1$, $p = 0.06$). When animals were assessed on post-injury days 28–31, brain-injured animals were significantly impaired in their ability to locate the hidden platform compared to sham-injured animals irrespective of treatment ($F_{(1,45)} = 8.6$, $p < 0.05$, Fig. 8C). In the probe trial, brain-injured animals spent less time in the platform zone compared to sham-injured animals ($F_{(1,15)} = 4.7$, $p < 0.05$, Fig. 8D) indicating a retention deficit. There was no effect of injury in the visible platform trial ($F_{(1,15)} = 2.0$, $p = 0.18$).

4. Discussion

Depletion of microglia within the site of maximal injury in the cortex led to increased staining for fluoro-Jade B (FJB) in both the acute (3 days) and chronic (35 days) post-injury periods compared to their empty liposome-injected counterparts. This increase in the number of FJB(+) profiles was associated with an increase in the amplitude of the extracellular evoked field potentials suggestive of altered neuronal circuity within the cortex. Depletion of microglia within the white matter tracts below the impact site did not reduce the extent of traumatic axonal injury but did lead to an increase in the number of FJB(+) profiles. Similarly, depletion of microglia led to an increase in FJB staining in both the thalamus and dorsal subiculum but did not exacerbate injury-induced spatial learning deficits at 4 weeks post-injury. Repopulation of microglia was almost complete by 35 days following depletion in both sham- and brain-injured animal although the ED-1(+) microglia in brain-injured animals continued to exhibit morphological signs of activation to a greater extent than those injected with empty liposome. Clodronate-induced microglia depletion in adult models of stroke or Alzheimer's models have been shown to be neuroprotective (Asai et al., 2015; Ma et al., 2016). In a model of hypothermic cardiac arrest in adult rats, clodronate administration effectively decreased the number of microglia in the hippocampus of injured rats but did not result in amelioration of neuronal cell death (Drabek et al., 2012). Collectively these data suggest that acute depletion of microglia may not be beneficial following TBI in the neonate.

Interestingly, the ED-1(+) microglia in brain-injured animals demonstrated both rod-like and amoeboid phenotypes. Rod-like microglia have been observed following TBI in the adult rat and our current study has identified that these microglia are an activated phenotype as evident by ED-1 immunoreactivity, but it is unclear whether or not they play a specific role in post-injury pathology (Taylor et al., 2014). There is some evidence to suggest that rod-like microglia are highly proliferative and can rapidly transformation to an amoeboid shape (Tam and Ma, 2014), suggesting that the rod-like microglia observed in the acute post-injury period in the clodronate-treated brain-injured animals may go on to become amoeboid microglia during the chronic post-traumatic period. To the best of our knowledge, this is the first reported case of rod-like microglial activation following experimental pediatric TBI. Further studies are needed to elucidate the functional role of rod-like microglia following trauma to the immature brain.

The temporal and regional patterns of microglia activation suggest that microglia are involved in injury-induced neurodegeneration. Both developmental and traumatic injury-induced cell death are associated with activation of microglia (Hanlon et al., 2016; Hanlon et al., 2017; Pont-Lezica et al., 2011; Simon et al., 2018; Tong et al., 2002). It is unclear, however, whether microglia actively initiate and/or perpetuate cell death or whether their role is to phagocytose dead/dying cells (Hanisch and Kettenmann, 2007; Loane and Kumar, 2016). Our observations of an increase in FJB labeling in clodronate-injected animals are similar to the exacerbation of lesion size and promotion of hemorrhage following stroke in the neonatal rat (Faustino et al., 2011; Fernandez-Lopez et al., 2016) although we did not observe any additional loss of cortical or thalamic area in the clodronate-injected brain-injured animals compared to their empty liposome-injected counterparts. Similarly, prolonged minocycline administration, an antibiotic that decreases microglial activation, also exacerbated neurodegeneration and caused a rebound increase in microglial reactivity during the chronic post-traumatic period following TBI in the neonate rat (Hanlon et al., 2017). We posit that the increase in FJB(+) profiles in clodronate-injected animals relative to those injected with empty liposomes may likely be a consequence of decreased phagocytosis of dying cells. Over the 4–5 weeks following injury, we did not observe any appreciable change in the extent of FJB staining in any injured brain region of the clodronate-injected animals. The concomitant observation that the repopulated microglia in these animals exhibited amoeboid (activated) morphology to a greater extent than those in empty liposome-injected brains may be representative of either a compensatory increase associated with the continued presence of degenerating neurons or the invasion of blood-borne macrophages. When neurodegeneration and microglial reactivity were increased in the hindlimb cortex region at the chronic post-traumatic period, the neuronal activity signals showed evidence of hyperactivity indicating dysfunction and disinhibition of neuronal circuitry. Further assessments are necessary to determine whether the hyperactivity in the local cortical circuitry is due to aberrant connections formed by the dying neurons and/or factors secreted from the activated microglia. We were unable to detect differences in the use of hindlimbs in the straight path swim test either as function of injury or injection of liposomes (data not shown) perhaps because of the predominant use of the hindlimbs to swim the straight path; neither injury nor liposome injection affected the speed at which the animals swam (data not shown). It must be noted that clodronate administration in the neonate rat induced a hyperlocomotive phenotype measured using open field behaviors (Nelson and Lenz, 2017; VanRyzin et al., 2016). Brain injury in the neonate resulted in hyperactivity within the forelimb region of the motor cortex which may be the basis for the disinhibition of the forelimb use in the straight path swim test (Stoltz et al., 1999). Injections of clodronate were localized to the hindlimb cortical region and the thalamus; therefore, it is not surprising that no effect of clodronate injection was observed on injury-induced hyperactivity in the forelimb region and the concomitant disinhibition of the forelimb function. The injection of clodronate into the thalamus allowed for diffusion into the dorsal subiculum leading to depletion of microglia in this region which may explain why sham-injured animals that received clodronate were unable to learn the location of the hidden platform during testing on days 10–14 and thereby suggesting that microglial activity may be necessary for normal cognitive functioning (Harry and Kraft, 2012; Schlegelmilch et al., 2011). Similarly, microglial depletion with clodronate at the early post-natal age induced chronic deficits in the T-maze, social recognition and novel object recognition tests (VanRyzin et al., 2016). Prolonged administration of minocycline following diffuse brain injury in the neonate rat exacerbated trauma-induced spatial memory deficits (Hanlon et al., 2017). Collectively, these data demonstrate that extremes of microglial activity- either too little or too excessive- may be detrimental for proper cognitive functioning of the immature brain following trauma. In contrast, a high dose of minocycline was able to reduce activation of microglia and improve spatial memory acquisition in brain-injured 17-day-old rats (Simon et al., 2018).

The observation that microglia depletion in the white matter does not affect the extent of traumatic axonal injury supports previous observations that minocycline treatment which decreased microglial activity in adult and pediatric TBI did not change the burden of axonal injury (Hanlon et al., 2016; Hanlon et al., 2017; Homsi et al., 2010). Similarly, genetic depletion of microglia did not alter silver staining, APP accumulation, or neurofilament labeling in the white matter tracts following repetitive brain injury in adult mice (Bennett and Brody, 2014). In the white matter tracts, microglia play a beneficial role in providing trophic support to oligodendrocyte precursor cells to aid them through differentiation into a mature myelinating

oligodendrocyte and therefore these cells share a very close spatial relationship (Domingues et al., 2016). When activated by an insult, microglia can be detrimental by inhibiting this maturation causing oligodendrocyte damage and myelination deficits (Domingues et al., 2016; Peferoen et al., 2014). Macrophage depletion with clodronate following demyelination injury in the adult rat impaired remyelination which was associated with a decreased expression of insulin-like growth factor 1 and a reduced oligodendrocyte progenitor cell response (Kotter et al., 2005). Oligodendrocyte death has been observed following TBI in adult rodents and hypoxic-ischemic (HI) injury in the neonate rat (Liu et al., 2002; Lotocki et al., 2011; Mierzwa et al., 2015). Future efforts need to determine whether the FJB profiles observed in the white matter tracts are indicative of both axonal fragments, dying oligodendrocytes and oligodendrocyte precursor cells.

Although clodronate depletes all Iba-1(+) cells at 3 days post-injury, ED-1(+) cells were observed in the regions of local depletion suggesting that these cells may reflect the infiltration of peripheral macrophages. At 35 days, the number of ED-1(+) cells in clodronate-injected brains were greater than that of Iba-1(+) profiles suggestive of differences in microglia population and underscore the importance of colabeling ED-1(+) cells with Iba-1, a limitation of the current study. In addition, the lack of observable sex differences may be reflective of being underpowered to detect significance. Despite these limitations, the data presented here demonstrate that microglia depletion following closed head injury in the neonate rat reduces clearance of degenerating neurons which was associated with increased neuronal activity but does not affect the extent of traumatic axonal injury and injury-induced motor and cognitive deficits. Further studies should focus on the cellular mechanisms underlying these responses and whether depleting microglia or inhibiting activation during the subacute and chronic post-traumatic periods provide greater benefit to the brain-injured animal.

Acknowledgements

The studies were supported, in part, by grants from the National Institutes of Health HD-061963 (RR, JWH) and a fellowship from the Biomedical Studies Graduate Student Association (LAH).

References

Abdel Baki, S.G., Schwab, B., Haber, M., Fenton, A.A., Bergold, P.J., 2010. Minocycline synergizes with N-acetylcysteine and improves cognition and memory following traumatic brain injury in rats. PLoS One 5, e12490.
Anderson, V., Catroppa, C., Morse, S., Haritou, F., Rosenfeld, J., 2005. Functional plasticity or vulnerability after early brain injury? Pediatrics 116, 1374–1382.
Anderson, V., Brown, S., Newitt, H., Hoile, H., 2009. Educational, vocational, psychosocial, and quality-of-life outcomes for adult survivors of childhood traumatic brain injury. J. Head Trauma Rehabil. 24, 303–312.
Anderson, V., Brown, S., Newitt, H., Hoile, H., 2011. Long-term outcome from childhood traumatic brain injury: intellectual ability, personality, and quality of life. Neuropsychology 25, 176–184.
Asai, H., Ikezu, S., Tsunoda, S., Medalla, M., Luebke, J., Haydar, T., Wolozin, B., Butovsky, O., Kugler, S., Ikezu, T., 2015. Depletion of microglia and inhibition of exosome synthesis halt tau propagation. Nat. Neurosci. 18, 1584–1593.
Babikian, T., Merkley, T., Savage, R.C., Giza, C.C., Levin, H., 2015. Chronic aspects of Pediatric traumatic brain injury: review of the literature. J. Neurotrauma 32, 1849–1860.
Bell, M.J., Kochanek, P.M., Doughty, L.A., Carcillo, J.A., Adelson, P.D., Clark, R.S., Wisniewski, S.R., Whalen, M.J., DeKosky, S.T., 1997. Interleukin-6 and interleukin-10 in cerebrospinal fluid after severe traumatic brain injury in children. J. Neurotrauma 14, 451–457.
Bennett, R.E., Brody, D.L., 2014. Acute reduction of microglia does not alter axonal injury in a mouse model of repetitive concussive traumatic brain injury. J. Neurotrauma 31, 1647–1663.
Berger, R.P., Heyes, M.P., Wisniewski, S.R., Adelson, P.D., Thomas, N., Kochanek, P.M., 2004. Assessment of the macrophage marker quinolinic acid in cerebrospinal fluid after pediatric traumatic brain injury: insight into the timing and severity of injury in child abuse. J. Neurotrauma 21, 1123–1130.
Beynon, S.B., Walker, F.R., 2012. Microglial activation in the injured and healthy brain: what are we really talking about? Practical and theoretical issues associated with the measurement of changes in microglial morphology. Neuroscience 225, 162–171.
Buttram, S.D., Wisniewski, S.R., Jackson, E.K., Adelson, P.D., Feldman, K., Bayir, H., Berger, R.P., Clark, R.S., Kochanek, P.M., 2007. Multiplex assessment of cytokine and chemokine levels in cerebrospinal fluid following severe pediatric traumatic brain injury: effects of moderate hypothermia. J. Neurotrauma 24, 1707–1717.
C.D.C, 2016. Injury Prevention & Control: Traumatic Brain Injury & Concussion: Rates of TBI-Related Emergency Department Visits, Hospitalizations, and Deaths - United States, 2001–2010.
Catroppa, C., Anderson, V., 2004. Recovery and predictors of language skills two years following pediatric traumatic brain injury. Brain Lang. 88, 68–78.
Catroppa, C., Anderson, V., 2006. Planning, problem-solving and organizational abilities in children following traumatic brain injury: intervention techniques. Pediatr. Rehabil. 9, 89–97.
Chhor, V., Moretti, R., Le Charpentier, T., Sigaut, S., Lebon, S., Schwendimann, L., Ore, M.V., Zuiani, C., Milan, V., Josserand, J., et al., 2017. Role of microglia in a mouse model of paediatric traumatic brain injury. Brain Behav. Immun. 63, 197–209.
Coronado, V.G., Xu, L., Basavaraju, S.V., McGuire, L.C., Wald, M.M., Faul, M.D., Guzman, B.R., Hemphill, J.D., 2011. Surveillance for traumatic brain injury-related deaths–United States, 1997-2007. MMWR Surveill. Summ. 60, 1–32.
Dennis, E.L., Ellis, M.U., Marion, S.D., Jin, Y., Moran, L., Olsen, A., Kernan, C., Babikian, T., Mink, R., Babbitt, C., et al., 2015. Callosal function in Pediatric traumatic brain injury linked to disrupted white matter integrity. J. Neurosci. 35, 10202–10211.
DiLeonardi, A.M., Huh, J.W., Raghupathi, R., 2009. Impaired axonal transport and neurofilament compaction occur in separate populations of injured axons following diffuse brain injury in the immature rat. Brain Res. 1263, 174–182.
Domingues, H.S., Portugal, C.C., Socodato, R., Relvas, J.B., 2016. Oligodendrocyte, astrocyte, and microglia crosstalk in myelin development, damage, and repair. Front. Cell Dev. Biol. 4, 71.
Drabek, T., Janata, A., Jackson, E.K., End, B., Stezoski, J., Vagni, V.A., Janesko-Feldman, K., Wilson, C.D., van Rooijen, N., Tisherman, S.A., et al., 2012. Microglial depletion using intrahippocampal injection of liposome-encapsulated clodronate in prolonged hypothermic cardiac arrest in rats. Resuscitation 83, 517–526.
Emami, P., Czorlich, P., Fritzsche, F.S., Westphal, M., Rueger, J.M., Lefering, R., Hoffmann, M., 2017. Impact of Glasgow Coma Scale score and pupil parameters on mortality rate and outcome in pediatric and adult severe traumatic brain injury: a retrospective, multicenter cohort study. J. Neurosurg. 126, 760–767.
Ewing-Cobbs, L., Prasad, M.R., Landry, S.H., Kramer, L., DeLeon, R., 2004. Executive functions following traumatic brain injury in young children: a preliminary analysis. Dev. Neuropsychol. 26, 487–512.
Ewing-Cobbs, L., Prasad, M.R., Kramer, L., Cox Jr., C.S., Baumgartner, J., Fletcher, S., Mendez, D., Barnes, M., Zhang, X., Swank, P., 2006. Late intellectual and academic outcomes following traumatic brain injury sustained during early childhood. J. Neurosurg. 105, 287–296.
Faul, M.D., Wald, Marlena M., Xu, Likang, Coronado, Victor G., 2010. Traumatic Brain Injury in the United States; Emergency Department Visits, Hospitalizations, and Deaths, 2002–2006. National Center for Injury Prevention and Control (U.S.), Division of Injury Response, Atlanta.
Faustino, J.V., Wang, X., Johnson, C.E., Klibanov, A., Derugin, N., Wendland, M.F., Vexler, Z.S., 2011. Microglial cells contribute to endogenous brain defenses after acute neonatal focal stroke. J. Neurosci. 31, 12992–13001.
Fernandez-Lopez, D., Faustino, J., Klibanov, A.L., Derugin, N., Blanchard, E., Simon, F., Leib, S.L., Vexler, Z.S., 2016. Microglial cells prevent Hemorrhage in neonatal focal arterial stroke. J. Neurosci. 36, 2881–2893.
Graeber, M.B., Streit, W.J., 2010. Microglia: biology and pathology. Acta Neuropathol. 119, 89–105.
Hanisch, U.K., Kettenmann, H., 2007. Microglia: active sensor and versatile effector cells in the normal and pathologic brain. Nat. Neurosci. 10, 1387–1394.
Hanlon, L.A., Huh, J.W., Raghupathi, R., 2016. Minocycline transiently reduces microglia/macrophage activation but exacerbates cognitive deficits following repetitive traumatic brain injury in the neonatal rat. J. Neuropathol. Exp. Neurol. 75, 214–226.
Hanlon, L.A., Raghupathi, R., Huh, J.W., 2017. Differential effects of minocycline on microglial activation and neurodegeneration following closed head injury in the neonate rat. Exp. Neurol. 290, 1–14.
Harry, G.J., Kraft, A.D., 2012. Microglia in the developing brain: a potential target with lifetime effects. Neurotoxicology 33, 191–206.
Homsi, S., Federico, F., Croci, N., Palmier, B., Plotkine, M., Marchand-Leroux, C., Jafarian-Tehrani, M., 2009. Minocycline effects on cerebral edema: relations with inflammatory and oxidative stress markers following traumatic brain injury in mice. Brain Res. 1291, 122–132.
Homsi, S., Piaggio, T., Croci, N., Noble, F., Plotkine, M., Marchand-Leroux, C., Jafarian-Tehrani, M., 2010. Blockade of acute microglial activation by minocycline promotes neuroprotection and reduces locomotor hyperactivity after closed head injury in mice: a twelve-week follow-up study. J. Neurotrauma 27, 911–921.
Kotter, M.R., Zhao, C., van Rooijen, N., Franklin, R.J., 2005. Macrophage-depletion induced impairment of experimental CNS remyelination is associated with a reduced oligodendrocyte progenitor cell response and altered growth factor expression. Neurobiol. Dis. 18, 166–175.
Kreutzberg, G.W., 1996. Microglia: a sensor for pathological events in the CNS. Trends Neurosci. 19, 312–318.
Kumamaru, H., Saiwai, H., Kobayakawa, K., Kubota, K., van Rooijen, N., Inoue, K., Iwamoto, Y., Okada, S., 2012. Liposomal clodronate selectively eliminates microglia from primary astrocyte cultures. J. Neuroinflammation 9, 116.
Lam, T.I., Bingham, D., Chang, T.J., Lee, C.C., Shi, J., Wang, D., Massa, S., Swanson, R.A., Liu, J., 2013. Beneficial effects of minocycline and botulinum toxin-induced constraint physical therapy following experimental traumatic brain injury. Neurorehabil. Neural Repair 27, 889–899.
Langlois, J.A., Rutland-Brown, W., Thomas, K.E., 2005. The incidence of traumatic brain injury among children in the United States: differences by race. J. Head Trauma Rehabil. 20, 229–238.

Lehenkari, P.P., Kellinsalmi, M., Napankangas, J.P., Ylitalo, K.V., Monkkonen, J., Rogers, M.J., Azhayev, A., Vaananen, H.K., Hassinen, I.E., 2002. Further insight into mechanism of action of clodronate: inhibition of mitochondrial ADP/ATP translocase by a nonhydrolyzable, adenine-containing metabolite. Mol. Pharmacol. 61, 1255–1262.
Liu, Y., Silverstein, F.S., Skoff, R., Barks, J.D., 2002. Hypoxic-ischemic oligodendroglial injury in neonatal rat brain. Pediatr. Res. 51, 25–33.
Loane, D.J., Kumar, A., 2016. Microglia in the TBI brain: the good, the bad, and the dysregulated. Exp. Neurol. 275 (Pt 3), 316–327.
Lotocki, G., de Rivero Vaccari, J., Alonso, O., Molano, J.S., Nixon, R., Dietrich, W.D., Bramlett, H.M., 2011. Oligodendrocyte vulnerability following traumatic brain injury in rats: effect of moderate hypothermia. Ther Hypothermia Temp Manag 1, 43–51.
Ma, Y., Li, Y., Jiang, L., Wang, L., Jiang, Z., Wang, Y., Zhang, Z., Yang, G.Y., 2016. Macrophage depletion reduced brain injury following middle cerebral artery occlusion in mice. J. Neuroinflammation 13, 38.
Mierzwa, A.J., Marion, C.M., Sullivan, G.M., McDaniel, D.P., Armstrong, R.C., 2015. Components of myelin damage and repair in the progression of white matter pathology after mild traumatic brain injury. J. Neuropathol. Exp. Neurol. 74, 218–232.
Nelson, L.H., Lenz, K.M., 2017. Microglia depletion in early life programs persistent changes in social, mood-related, and locomotor behavior in male and female rats. Behav. Brain Res. 316, 279–293.
Newell, E., Shellington, D.K., Simon, D.W., Bell, M.J., Kochanek, P.M., Feldman, K., Bayir, H., Aneja, R.K., Carcillo, J.A., Clark, R.S., 2015. Cerebrospinal fluid markers of macrophage and lymphocyte activation after traumatic brain injury in children. Pediatr. Crit. Care Med. 16, 549–557.
Nimmerjahn, A., Kirchhoff, F., Helmchen, F., 2005. Resting microglial cells are highly dynamic surveillants of brain parenchyma in vivo. Science 308, 1314–1318.
Peferoen, L., Kipp, M., van der Valk, P., van Noort, J.M., Amor, S., 2014. Oligodendrocyte-microglia cross-talk in the central nervous system. Immunology 141, 302–313.
Pont-Lezica, L., Bechade, C., Belarif-Cantaut, Y., Pascual, O., Bessis, A., 2011. Physiological roles of microglia during development. J. Neurochem. 119, 901–908.
Power, T., Catroppa, C., Coleman, L., Ditchfield, M., Anderson, V., 2007. Do lesion site and severity predict deficits in attentional control after preschool traumatic brain injury (TBI)? Brain Inj. 21, 279–292.
Pullela, R., Raber, J., Pfankuch, T., Ferriero, D.M., Claus, C.P., Koh, S.E., Yamauchi, T., Rola, R., Fike, J.R., Noble-Haeusslein, L.J., 2006. Traumatic injury to the immature brain results in progressive neuronal loss, hyperactivity and delayed cognitive impairments. Dev. Neurosci. 28, 396–409.
Raghupathi, R., Huh, J.W., 2007. Diffuse brain injury in the immature rat: evidence for an age-at-injury effect on cognitive function and histopathologic damage. J. Neurotrauma 24, 1596–1608.
Ransohoff, R.M., Perry, V.H., 2009. Microglial physiology: unique stimuli, specialized responses. Annu. Rev. Immunol. 27, 119–145.
Salorio, C.F., Slomine, B.S., Grados, M.A., Vasa, R.A., Christensen, J.R., Gerring, J.P., 2005. Neuroanatomic correlates of CVLT-C performance following pediatric traumatic brain injury. J. Int. Neuropsychol. Soc. 11, 686–696.
Sangobowale, M.A., Grin'kina, N.M., Whitney, K., Nikulina, E., St Laurent-Ariot, K., Ho, J.S., Bayzan, N., Bergold, P.J., 2018. Minocycline plus N-acetylcysteine reduce Behavioral deficits and improve histology with a clinically useful time window. J. Neurotrauma.
Schlegelmilch, T., Henke, K., Peri, F., 2011. Microglia in the developing brain: from immunity to behaviour. Curr. Opin. Neurobiol. 21, 5–10.
Simon, D.W., Aneja, R.K., Alexander, H., Bell, M.J., Bayir, H., Kochanek, P.M., Clark, R.S.B., 2018. Minocycline attenuates high mobility group box 1 translocation, microglial activation, and thalamic Neurodegeneration after traumatic brain injury in post-Natal day 17 rats. J. Neurotrauma 35, 130–138.
Siopi, E., Cho, A.H., Homsi, S., Croci, N., Plotkine, M., Marchand-Leroux, C., Jafarian-Tehrani, M., 2011. Minocycline restores sAPPalpha levels and reduces the late histopathological consequences of traumatic brain injury in mice. J. Neurotrauma 28, 2135–2143.
Siopi, E., Calabria, S., Plotkine, M., Marchand-Leroux, C., Jafarian-Tehrani, M., 2012. Minocycline restores olfactory bulb volume and olfactory behavior after traumatic brain injury in mice. J. Neurotrauma 29, 354–361.
Stoltz, S., Humm, J.L., Schallert, T., 1999. Cortical injury impairs contralateral forelimb immobility during swimming: a simple test for loss of inhibitory motor control. Behav. Brain Res. 106, 127–132.
Tam, W.Y., Ma, C.H., 2014. Bipolar/rod-shaped microglia are proliferating microglia with distinct M1/M2 phenotypes. Sci. Rep. 4, 7279.
Taylor, S.E., Morganti-Kossmann, C., Lifshitz, J., Ziebell, J.M., 2014. Rod microglia: a morphological definition. PLoS One 9, e97096.
Tong, W., Igarashi, T., Ferriero, D.M., Noble, L.J., 2002. Traumatic brain injury in the immature mouse brain: characterization of regional vulnerability. Exp. Neurol. 176, 105–116.
Tong, K.A., Ashwal, S., Holshouser, B.A., Nickerson, J.P., Wall, C.J., Shutter, L.A., Osterdock, R.J., Haacke, E.M., Kido, D., 2004. Diffuse axonal injury in children: clinical correlation with hemorrhagic lesions. Ann. Neurol. 56, 36–50.
van Rooijen, N., van Kesteren-Hendrikx, E., 2003. “In vivo” depletion of macrophages by liposome-mediated “suicide”. Methods Enzymol. 373, 3–16.
VanRyzin, J.W., Yu, S.J., Perez-Pouchoulen, M., McCarthy, M.M., 2016. Temporary depletion of microglia during the early postnatal period induces lasting sex-dependent and sex-independent effects on behavior in rats. eNeuro 3.
Wallisch, J.S., Simon, D.W., Bayir, H., Bell, M.J., Kochanek, P.M., Clark, R.S.B., 2017. Cerebrospinal fluid NLRP3 is increased after severe traumatic brain injury in infants and children. Neurocrit. Care. 27, 44–50.
Whalen, M.J., Carlos, T.M., Kochanek, P.M., Wisniewski, S.R., Bell, M.J., Clark, R.S., DeKosky, S.T., Marion, D.W., Adelson, P.D., 2000. Interleukin-8 is increased in cerebrospinal fluid of children with severe head injury. Crit. Care Med. 28, 929–934.
Wilde, E.A., Hunter, J.V., Newsome, M.R., Scheibel, R.S., Bigler, E.D., Johnson, J.L., Fearing, M.A., Cleavinger, H.B., Li, X., Swank, P.R., et al., 2005. Frontal and temporal morphometric findings on MRI in children after moderate to severe traumatic brain injury. J. Neurotrauma 22, 333–344.
Woodcock, T., Morganti-Kossmann, M.C., 2013. The role of markers of inflammation in traumatic brain injury. Front. Neurol. 4, 18.
Zhang, Z., Saraswati, M., Koehler, R.C., Robertson, C., Kannan, S., 2015. A new rabbit model of Pediatric traumatic brain injury. J. Neurotrauma 32, 1369–1379.